HiSST: International Conference on
High-Speed Vehicle Science Technology
26–29 November 2018, Moscow, Russia

Mathematical simulation, numerical and experimental investigation of nonspherical bodies' motion in nonuniform flows

Ivan A. Amelyushkin (Central Aerohydrodynamic Institute)

Abstract

The complexity of mathematical modeling of nonstationary dynamics of multiple bodies in inhomogeneous flows and the significant stochastic nature of their trajectories in gradient media under experimental investigation lead to construction of original approaches in mathematical and numerical simulation of the dynamics of chaotic clouds of bodies of complex shapes. Results of shape influence on trajectories' stochastic and spreading of nonspherical bodies in gradient flows are obtained and presented in terms of dimensionless governing parameters. Algorithms for determination gas parameters via particles' motion analysis are developed.

Keywords: *nonspherical bodies, non-uniform flow, stochastic motion, non-intrusive optical diagnostics*

Nomenclature

Latin
Re - Reynolds number
M - Mach number
$\boldsymbol{F}$ - force vector
S - scattering coefficient
q - flux
$\boldsymbol{e}$ - unity vector
e - specific energy density
a - big simiaxes of spheroid
b - small simiaxes of spheroid, impingement parameter
a_p - volumetrically equivalent particle's radius
C - coefficient
$\boldsymbol{V}$ - velocity vector
V - velocity module
$\hat{\boldsymbol{P}}$ - tensor of tension
$\hat{\boldsymbol{S}}$ - strain rate tensor
$\hat{\boldsymbol{E}}$ - unity matrix
d - coefficient in linear tensor equation
u - x velocity component
v - y velocity component
f - force coefficients
E - shape parameter
F_X - root-mean-square force deviation
R - circumfluent body's radius, gas constant
m - mass
W - energy density
t - time
k - constant, kinetic energy density of turbulent pulsations
T - temperature
L - characteristic size
Nu - Nusselt number
Pr - Prandtl number

Greek
φ - orientation force coefficient
χ - chaotization
ρ - density
α - angle of attack
σ - surface tension coefficient
τ - time
μ - dynamic gas viscosity
τ - characteristic time
Ξ - random unity vector
Γ -stabilization coefficient

Superscripts
V - volumetric
0 - initial
Stk - Stokes
NS - nonspherical

Subscripts
p - particle
A - average
|| - parallel, longitude
$\perp$ - perpendicular, transverse
x - x component

y - y component
Stk - Stokes
∞ - far away from perturbation area
a_p - particle's radius
D - drag
k - number of stohastics' type
B - Boltsman
Br - Brownian
NS - nonspherical
Turb - turbulent
Det - deterministic
R - relaxation
0 - initial
F - flow

1. Introduction

Multiphase flows are widespread in nature and human practice. Aircraft safety and ice accretion simulation are important problems in aeronautical sciences [1,2]. Present paper concerns nonspherical particles [3-5] with application for aircraft icing investigations. Flight in mixed (droplets/crystals) clouds is accompanied by many physical processes – trajectory bounding of solid or liquid particles, their impingement upon a surface, bouncing or damage, mutual collisions, etc.
The role of water crystals orientation is investigated in nonsymmetrical impingement upon transversal cylinder. The correspondent numerical analysis was developed for small Reynolds numbers (especially in microaviation application) as well as for large those, on the basis of the spheroid model of crystal.
In previous publications original algorithms were proposed to determine two phase flow parameters in wind tunnels via laser sheet images analysis [6,7], optical system for aerosol flow with ice crystal and supercooled droplets' was developed as well as corresponding methods of flow visualization and image processing. Peculiarities of supercooled droplets and nonspherical ice crystal interaction [5,8,9] with a solid body were investigated via molecular dynamics and Lagrangian mechanics technique.
Simulation of the nonstationary motion of bodies of complex shape in inhomogeneous media, particles of natural origin, nanodispersed flows where thermal fluctuations are significant, as well as the various effects in dusty plasmas, is of great scientific and practical interest in a wide range of fields of technology, economy, nature and life of human beings. Previous studies [2,5] demonstrate influence of particles' shape on two-phase flow near a circumfluent body characteristics, in particular, on mass flow rate surface distribution, which is essential for aircraft icing calculation.

2 MATHEMATICAL SIMULATION OF NONSPHERICAL PARTICLES' MOTION

2.2 Theoretical calculation of mean and orientation forces

In spite of a lot of different mathematical models for aerohydrodynamic characteristics of single nonspherical particles' (e.g. [3-5]), simulation of the whole two-phase flow with nonspherical particles becomes problematic [6,7]. In order to calculate scattering coefficient of nonspherical particles and orientational force in nonuniform flows let us calculate an average force, which acts on a particle.
An attempt to introduce an orientational force for the two-dimensional motion of spheroids was undertaken in [2] by analogy with orientational forces in molecular dynamics [10]. For small Reynolds numbers of particles motion in a carrying media reference frame there is the following expression [5] for the force which acts on spheroids:

$$\boldsymbol{F}(\mathrm{Re}_p) = \frac{\rho\pi a_p^2}{2}\frac{24}{\mathrm{Re}_p}\left|\boldsymbol{V}-\boldsymbol{V}_p\right|\left[f_{\parallel}\left(\boldsymbol{V}-\boldsymbol{V}_p\right)_{\parallel} + f_{\perp}\left(\boldsymbol{V}-\boldsymbol{V}_p\right)_{\perp}\right] = 3\pi\frac{\mu^2}{\rho}\mathrm{Re}_p\left[f_{\parallel}\cos\theta\boldsymbol{i}_{\parallel} + f_{\perp}\sin\theta\boldsymbol{i}_{\perp}\right]$$

Here $\boldsymbol{V}$ – gas velocity in a point of spheroid's mass center, $\boldsymbol{V_p}$ – spheroid's center of mass velocity. In the above expression the first term – "drag force", the second one – lift force.

In these terms correction multipliers to velocity components are described by following expressions for quasi Stokes gas circumfluent of a particle.

For longitude spheroid ($E > 1$) force coefficients will be as follows:

$$f_{\parallel} = \frac{4}{3}\frac{\left(E^2-1\right)^{3/2}}{E^{1/3}}\frac{1}{\left(2E^2-1\right)\ln\left(E+\sqrt{E^2-1}\right)-E\sqrt{E^2-1}},\quad f_{\perp} = \frac{8}{3}\frac{\left(E^2-1\right)^{3/2}}{E^{1/3}}\frac{1}{\left(2E^2-3\right)\ln\left(E+\sqrt{E^2-1}\right)+E\sqrt{E^2-1}}.$$

For oblate spheroid ($E < 1$):

$$f_{\parallel} = \frac{4}{3}\frac{\left(1-E^2\right)^{3/2}}{E^{1/3}}\frac{1}{E\sqrt{1-E^2}+\left(1-2E^2\right)\arccos E},\ f_{\perp} = \frac{8}{3}\frac{\left(1-E^2\right)^{3/2}}{E^{1/3}}\frac{1}{\left(3-2E^2\right)\arccos E - E\sqrt{1-E^2}}.$$

In present study complex shape particles are simulated via spheroids (fig. 1) with the characteristic governing parameter $E = d_{\parallel}/d_{\perp} = a/b$, and volumetrically equivalent radius: $a_p = bE^{1/3} = a/E^{2/3}$, $d_{\parallel} = 2a = 2a_p E^{2/3}$, $d_{\perp} = 2a_p/E^{1/3}$.

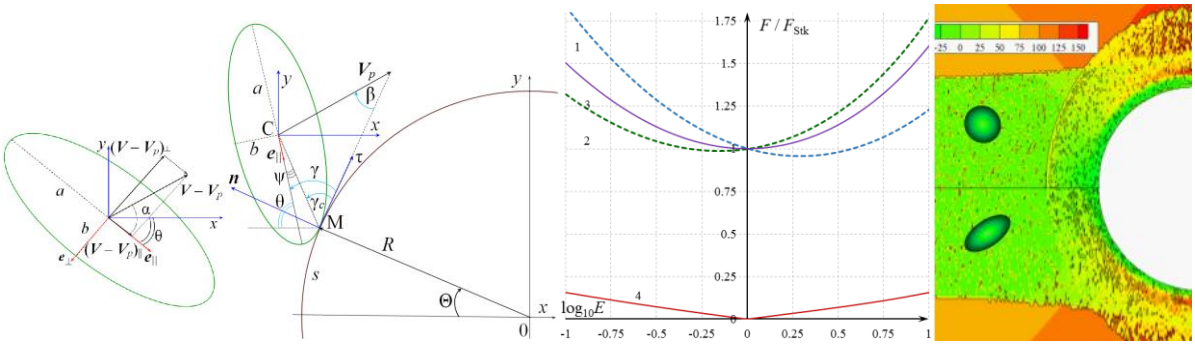

Fig. 1. Scheme of spheroid's motion towards circumfluent body and it's collision with a transversal cylinder's surface, *a*, *b* – sizes of nonspherical particle; α, β – angles of attack and slipping angle; ***V*–*V*$_p$** – velocity of gas flow in a reference frame with a particle, $\boldsymbol{e}_{\parallel}$ – unity vector which is directed along spheroid's symmetry axis. In a center: Dependence of coefficients of a force which act on nonspherical particle: 1 – $f_{\parallel}(E)$, 2 – $f_{\perp}(E)$, 3 – average force coefficient $f_A(E)$ and 4 – orientational force coefficient $\varphi(E)$. On the right: velocity nonequilibrium comparison for a flow with spherical and volumetrically equivalent nonspherical (E=3) particles.

$$\frac{<\boldsymbol{F}(\mathrm{Re}_p)>}{3\pi\left(\mu^2/\rho\right)\mathrm{Re}_p} = f_A = \frac{1}{2\pi}\int_0^{\pi/2} 2\pi\sin\theta\sqrt{f_{\parallel}^{\,2}\cos^2\theta + f_{\perp}^{\,2}\sin^2\theta}\,d\theta =$$

$$= \frac{f_{\perp}^{\,2}}{4\sqrt{f_{\parallel}^{\,2}-f_{\perp}^{\,2}}}\left(-\ln\left(\frac{f_{\perp}^{\,2}}{f_{\parallel}^{\,2}-f_{\perp}^{\,2}}\right)+2\left[\frac{f_{\parallel}}{f_{\perp}^{\,2}}+\sqrt{f_{\parallel}^{\,2}-f_{\perp}^{\,2}}\ln\left(1+\sqrt{\frac{f_{\parallel}^{\,2}}{f_{\parallel}^{\,2}-f_{\perp}^{\,2}}}\right)\right]\right)$$

The mean deviation square from the average force is described by the following expression:

$$\left(\frac{F_{\chi}}{F_{\mathrm{Stk}}}\right)^2 = \left(\frac{\delta\boldsymbol{F}(\mathrm{Re}_p,\mathrm{M})}{3\pi\left(\mu^2/\rho\right)\mathrm{Re}_p}\right)^2 = \frac{1}{2\pi}\int_0^{\pi/2} 2\pi\sin\theta\left[f_A - \sqrt{f_{\parallel}^{\,2}\cos^2\theta + f_{\perp}^{\,2}\sin^2\theta}\right]^2 d\theta = -f_A^{\,2} + \frac{f_{\parallel}^{\,2}+2f_{\perp}^{\,2}}{3} = \varphi^2$$

Expressions for $f_{\parallel}$ and $f_{\perp}$ in general and simplified forms one can find in [5]. Values of force coefficients dependency on shape parameter E are shown in fig. 1 (in a center), force components' coefficients (curve 1 and 2), average force component (curve 3) and orientation force component (curve 4). The expression for orientation force one may use for particles' scattering simulation in velocity nonequilibrium two-phase flows.

2.2 Influence of particle shape on particles on solid body impacting region size

Particles' stochastic motion affects peculiarities of a flow near a circumfluent body. In particular, particles' deviations from deterministic trajectories may increase a region of inertial particles' impingement [5]. Particles' velocity is a sum of deterministic velocity $\boldsymbol{V}_p^0$ and sum of stochastic motion velocities.

$$\boldsymbol{V}_p = \boldsymbol{V}_p^0 + \frac{|\boldsymbol{V}'|}{\sqrt{1+t/\tau_R}}\cdot\boldsymbol{\Xi}_{\mathbf{Turb}} + \sqrt{\frac{8k_B T}{\pi m_1 N}}\cdot\boldsymbol{\Xi}_{\mathbf{Br}} + V_{\mathrm{NS}}\cdot\boldsymbol{\Xi}_{\mathbf{NS}}$$

There are various mechanisms of particles' stochastic motion: receptivity for turbulent pulsations (second term) Brownian motion (third term) and forces which are due to nonspherical particles' orientation (the last term). It should be noted, that there could be other mechanisms of particles'

stochastic motion (e.g. fluctuations of electric field) but they are not taken into account in present study because of their negligible values.

In fig. 2 (in the left) one can see particles deterministic trajectories (red lines), carrying them gas flow lines and shema of partcles' stohastic motion mechanism superposition. The following expression may be used for impingement parameter $b_{\max}$ (fig. 2) estimations, which depends on receptvity to turbulent pulasations, brownian fluctuations and also on particles' nonspherical shape which may lead to additional particles' scattering:

$$\left(\frac{b_{\max}}{R}\right)^2 = \left(\frac{\mathrm{Stk}}{1+\mathrm{Stk}}\right)^2 + \frac{2D_t}{RV_\infty}\frac{1}{\sqrt{1+\mathrm{Stk}\cdot\tau_R/\tau_t}} + \frac{2D_{\mathrm{Br}}}{RV_\infty} + \frac{2S_\chi}{RV_\infty}$$

Here R – is a cylinder radius which simulates the leading age of the wing, u_∞ – flow velocity at a distance which is far away from the circumfluent body.

$\tau_R = (8/3)(\rho/\rho_p)(a_p/V_\infty)/C_D$ – time of particles' motion relaxation (characteristic time when particles' velocity becomes approximately equal carrying them gas velocity); C_D – particles' drag coefficient which at small Reynolds numbers Re_p of particles' motion relatively carrying gas media tends to $C_D^{\mathrm{St}} = 24/\mathrm{Re}_p$, where $\mathrm{Re}_p = \rho 2a_p V_\infty/\mu$. D_t – coefficient of turbulent diffusion which is connected with energy of carrying gas turbulent pulsations k and corresponding velocity of their dissipation ε by the following expression $D_t = 0.19k^2/\varepsilon$; $D_{\mathrm{Br}} = \mathrm{k_B}T/\mu a_p$ – κcoefficient of particles' diffusion due to Brownian migration; $S_\chi = \sqrt{\varphi(E)6\pi\mu a_p V_\infty/\rho_p}$, Stk – parameter which characterizes aerosol flow velocity nonequilibrium which depends on flow conditions: $\mathrm{Stk} = \mathrm{Stk}_0\left[C_D/(24/\mathrm{Re}_p)\right]\exp(-0.03\cdot\mathrm{We})$. Here $\mathrm{We} = \rho 2a_p V_\infty^2/\sigma$ – is a Weber number. At high speed of a liquid particle motion in a reference frame, connected with carrying gas, droplet deforms and it's drag become smaller. It leads to extremums in dependency of region at a surface where particles collide with a sircumfluent body on particles' radius and Stokes number: $\mathrm{Stk}_0 = \frac{2\rho_p V_\infty}{9\mu R}a_p^2$.

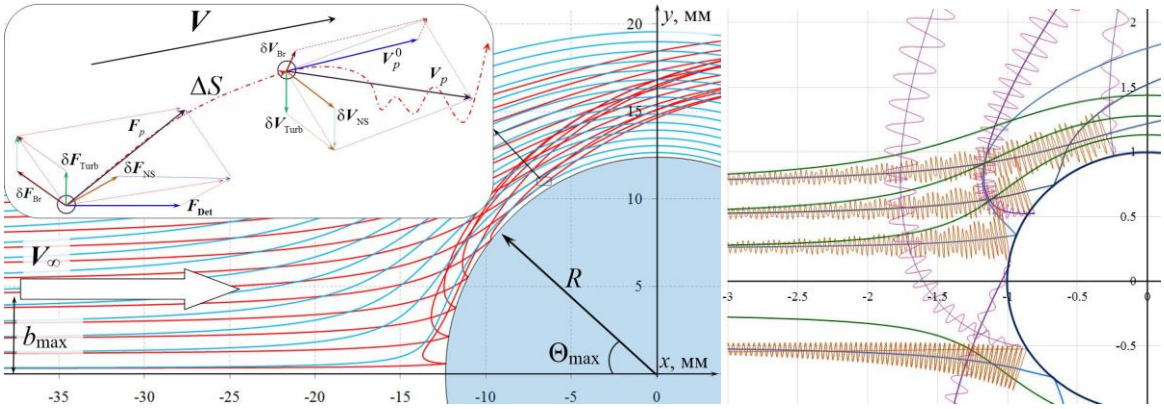

Fig 2. Scheme of particles' motion near the cross cylinder. Red lines – particles' deterministic trajectories, line with dots schematically shows particles' stochastic motion. On the right: qualitive scheme of nonspherical particles trajectories' fluctuations near a cross cylinder.

3 CONTINUUM MECHANICS EQUATIONS FOR STOHASTIC MOTION OF NONSOHERICAL BODIES DESCRIPTION

3.1 Mathematical simulation of nonspherical particles' motion in terms of continuum mechanics equations

As was mentioned above, nonspherical particles' scattering leads to modification of two phase flow governing equations. Particles' scattering leads to additional mass flow in equations of flow motion: $\boldsymbol{q}_\chi = S_\chi(\rho_p^V + \rho)\overline{\nabla}\left(\frac{\rho_p^V}{\rho_p^V + \rho}\right) \to S_\chi\overline{\nabla}\rho_p^V$. Here $S_\chi = \sqrt{F_\chi/\rho_p}$. Thus corresponding equations for particles and carrying them flow will be the following –

Mass conservation equations: $\frac{\partial \rho}{\partial t} + \left(\overline{\nabla} \cdot \rho \boldsymbol{V}\right) = 0$, $\frac{\partial \rho_p^V}{\partial t} + \left(\overline{\nabla} \cdot \rho_p^V \boldsymbol{V}_p\right) = \boldsymbol{q}_\chi$

Momentum equations: $\rho \frac{\mathrm{d}\boldsymbol{V}}{\mathrm{d}t} = \overline{\nabla} \cdot \hat{\boldsymbol{P}} - \frac{\rho_p^V}{m_p^0} \boldsymbol{F}_p$ $\rho_p^V \frac{\mathrm{d}\boldsymbol{V}_p}{\mathrm{d}t} = \frac{\rho_p^V}{m_p^0} \boldsymbol{F}_p + \overline{\nabla} \boldsymbol{q}_\chi \boldsymbol{V}_p$

And energy balance equations:

$$\rho \frac{\mathrm{d}e}{\mathrm{d}t} = \overline{\nabla}\, \hat{\boldsymbol{P}} \boldsymbol{V} + \overline{\nabla}\left(\lambda(n_p) \overline{\nabla} T\right) - \frac{\rho_p^V}{m_p^0} \boldsymbol{F}_p \cdot \left(\boldsymbol{V} - \boldsymbol{V}_p\right) - \frac{\rho_p^V}{m_p^0} Q_p,$$

$$\rho_p^V \frac{\mathrm{d}e_p}{\mathrm{d}t} = \frac{\rho_p^V}{m_p^0} \boldsymbol{F}_p \cdot \left(\boldsymbol{V} - \boldsymbol{V}_p\right) + \overline{\nabla} \boldsymbol{q}_\chi \frac{\boldsymbol{V}_p^2}{2} + \frac{\rho_p^V}{m_p^0} Q_p.$$

Here $\boldsymbol{F}_p$ – is a deterministic force which acts on volumetrically equivalent sphere e_p – particles' energy density. $Q_p = 2\pi a \lambda \left(T(a) - T_\infty\right) \mathrm{Nu}(\mathrm{Re}_p, \mathrm{Pr})$. $\hat{\boldsymbol{P}} = 2\mu \hat{\boldsymbol{S}} + d\, \hat{\boldsymbol{E}}$, $d = -P - \frac{2\mu}{3} \overline{\nabla} \cdot \boldsymbol{V}$.

$$\boldsymbol{F}_p = \frac{c_D(\mathrm{Re}_p)}{24/\mathrm{Re}_p} 3\pi\mu a_p \left(\boldsymbol{V} - \boldsymbol{V}_p\right) + m_p \boldsymbol{g}\left(1 - \frac{\rho}{\rho_p}\right) + m_p \frac{\rho}{\rho_p} \frac{\mathrm{d}\left(\boldsymbol{V} - \boldsymbol{V}_p\right)}{\mathrm{d}t} + 6a_p^2 \sqrt{\pi\rho\mu} \int_{-\infty}^{t} \frac{1}{\sqrt{t-\tau}} \frac{\mathrm{d}\left(\boldsymbol{V} - \boldsymbol{V}_p\right)}{\mathrm{d}\tau} \mathrm{d}\tau +$$

$$+ 4.46 a_p^2 \sqrt{\mu\rho \left|\frac{\partial u_\parallel}{\partial y_\perp}\right|} \left(\boldsymbol{V}_p - \boldsymbol{V}\right) \mathrm{sign}\left(\frac{\partial u_\parallel}{\partial y_\perp}\right) + \Sigma \boldsymbol{F}$$

Here the first term is drag force, the second one is superposition of gravity and bouancy force, third one inheritant Basset force, the last but one – Saffman lift force and the last term describes superposition of forces which are not connected with aerohydrodynamics.

These equations may be used for taking into account nonspherical shape scattering effects in two-phase flows simulation in practical applications: high speed vehicles' motion in dusty atmospheres, aerosol flow with nonspherical ice crystals, transport of nature origin particles, etc.

Table 1. Dimensionless parameters of nonspherical particles' motion

Physical quantity	Nondimensional expression
Orientation force	$F_\chi / F_{\mathrm{Stk}} = \varphi$
Scattering coefficient	$\frac{S_\chi}{\mu/\rho} = \frac{\rho}{\mu} \sqrt{\frac{F_\chi}{\rho_p}} = \sqrt{\frac{\rho}{\rho_p}} \sqrt{3\pi \mathrm{Re}_p \varphi}$
Velocity	$\frac{V_\chi}{V_\infty} = \mathrm{Re}_\infty \frac{L}{a_p} \sqrt{\frac{\rho}{\rho_p}} \sqrt{\mathrm{Re}_p \varphi \left(\frac{243}{16}\pi\right)^{1/6}}$
Length	$\frac{A_\chi}{a_p} = \frac{1}{3} \sqrt{\frac{\rho_p}{\rho}} \sqrt{\frac{\mathrm{Re}_p}{\varphi}} \frac{(4\pi/3)^{1/6}}{\mathrm{Re}_\infty^2}$
Frequency	$\frac{\omega_\chi a_p}{V_\infty} = \frac{1}{\mathrm{Re}_\infty} \frac{L}{a_p} \sqrt{\frac{\rho}{\rho_p}} \sqrt{\mathrm{Re}_p \varphi} \frac{3}{2} \left(\frac{3}{4\pi}\right)^{1/6}$
Stabilization coefficient	$\frac{\Gamma_\chi}{\rho V_\infty \pi a_p^2 / 2} = 4 \left(\frac{3}{4\pi}\right)^{1/6} \sqrt{\frac{\rho_p}{\rho} \varphi \mathrm{Re}_p} \frac{h}{a_p} \frac{1}{\mathrm{Re}_\infty}$
Pressure	$\frac{P_\chi}{\rho V_\infty^2} = \frac{\rho_p^V}{\rho_p} \left(\frac{\mathrm{Re}_\infty h}{a_p}\right)^2 \mathrm{Re}_p \varphi \left(\frac{243}{16}\pi\right)^{1/3}$

3.2 Equation of nonspherical bodies' chaotic motion in nonuniform flows

The complexity of mathematical modeling of nonstationary dynamics of multiple bodies in inhomogeneous flows and the pronounced probabilistic nature of their trajectories in gradient media under experimental investigation leaded to the construction of original approaches in mathematical and numerical simulation of the dynamics of chaotic clouds of bodies of complex shapes. The equation for the change in the chaotic energy W_χ of nonspherical particles under the assumption that there are no phase transitions and temperature nonequilibrium is the following:

$$\frac{\partial W_\chi}{\partial t} + (\boldsymbol{V} - \boldsymbol{V}_p)\overline{\nabla} W_\chi = \frac{F_\chi \cdot V_\chi}{m_p} - \Gamma_\chi V_\chi \left| \boldsymbol{V} - \boldsymbol{V}_p \right|.$$

The first term in the right describes the production of chaotic energy, the second one describes the dissipation of this energy. Table 1 illustrates the calculated parameters of the gas (chaos) of nonspherical particles in inhomogeneous flows in a dimensionless form.

4 OPTICAL INVESTIGATION OF HIGH SPEED TWO-PHASE AEROSOL FLOWS

The information about the dispersed phase behavior (of particles) allows to determine a variety of fluid and gas flow parameters. Main methods of velocity measuring on particles images are PIV (Particle Image Velocimetry), PTV (Particle Tracking Velocimetry), LDA (Laser Doppler Anemometry). The gas velocity is determined indirectly by velocity of light diffusing (tracing) particles or their clusters, naturally been present in the flow or specially introduced into it. Thus, the assumption that the particles velocity equals to the velocity of the carrier flow is used. This assumption is justified in many practical problems. However, in the rarefied or high-gradient flows (for example, in supersonic flows in shock wind tunnels [6,7]), diagnosing of coarse-dispersed flows [9], two-phase flow velocity equilibrium may be significantly disrupted.

In some expensive aerophysical experiments, particularly in high supersonic wind tunnels, the running time of which is small, and the cost of experiment is large, the problem of diagnostic information capability increasing is extremely vital problem.

Accounting of two-phase flow velocity nonequilibrium in order to increase the accuracy of tracing anemometry was considered earlier in [7].

The simplest way of gas velocity field (which may significantly differ from particles velocity field in high speed flows) correction could be connected with well-known Stokes's *Cd* – drag coefficient model ($Cd = 24/\mathrm{Re}_p$) which could be applied for small differences between particle and gas velocities, and as result small Reynolds numbers $\mathrm{Re}_p = 2a_p|\boldsymbol{V}-\boldsymbol{V_p}|/\mu$ both for stationary and non-stationary flows. Here $\boldsymbol{V}$ and $\boldsymbol{V_p}$ – velocity vectors of gas and particles, ρ_p and a_p – particle's material density and its average radius, μ – dynamic gas viscosity. In this case because of small influence of temperature on particle motion in the gas in most practical tasks there is no need to calculate density field and the correction procedure may be expressed by the following equation: $\boldsymbol{V} = \boldsymbol{V_p} + \left[\frac{\partial \boldsymbol{V}_p}{\partial t} + (\boldsymbol{V}_p \cdot \overline{\nabla})\boldsymbol{V}_p\right]\frac{2\rho_p a_p^2}{9\mu(T)}\zeta$. Here ζ is a coefficient which takes into account particles shape. It should be noted that here V_p – is particles' velocity which is composed from deterministic and stochastic parts of velocities. Expression for temperature field estimation in high speed flow in a stationary case one may derive from the energy balance equation in a stationary flow:

$$\overline{\nabla}\left(\rho\boldsymbol{V}\left(C_p T + \frac{|\boldsymbol{V}|^2}{2}\right) - \mu\overline{\nabla}\left(\frac{C_p T}{\mathrm{Pr}} + \frac{|\boldsymbol{V}|^2}{2}\right) - \mu\cdot\mathrm{rot}\boldsymbol{V}\times\boldsymbol{V} + \frac{2}{3}\mu\boldsymbol{V}\cdot\overline{\nabla}\boldsymbol{V}\right) = 0$$

Taking the assumption that $V_{||} >> V_\perp$ and $\partial/\partial x_{||} >> \partial/\partial x_\perp$, after integrating the above expression, multiplying on velocity vector $\boldsymbol{V}$, using mass conservation equation $\overline{\nabla}\rho\boldsymbol{V} = 0$ for stationary case, using perfect gas equation of state, expressing C_P as $C_p = R\gamma/(\gamma-1)$, excluding pressure gradient by using momentum balance equation $(\boldsymbol{V}\cdot\overline{\nabla})\boldsymbol{V} = -\frac{\overline{\nabla}P}{\rho} + 2\frac{\mu}{\rho}\left[\overline{\nabla}\hat{\boldsymbol{S}} - \frac{1}{3}\overline{\nabla}\left(\overline{\nabla}\boldsymbol{V}\cdot\hat{\boldsymbol{E}}\right)\right]$, with the help of Gromeka-Lamb expression $(\boldsymbol{V}\cdot\overline{\nabla})\boldsymbol{V} = \overline{\nabla}\frac{|\boldsymbol{V}|^2}{2} + \mathrm{rot}\boldsymbol{V}\times\boldsymbol{V}$ and taking in account zero scalar product of perpendicular

vectors $\boldsymbol{V}\cdot\mathrm{rot}\boldsymbol{V}\times\boldsymbol{V}=0$ the expression for temperature field distribution estimation via PIV velocity field analysis in a stationary flow will become the following:

$$T=\frac{\rho_\infty(\boldsymbol{V}\cdot\boldsymbol{V}_\infty)\left(RT_\infty-(\gamma-1)\frac{|\boldsymbol{V}|^2-|\boldsymbol{V}_\infty|^2}{2\gamma}\right)+\frac{2}{\mathrm{Pr}}\frac{\mu^2}{\rho}\boldsymbol{V}\left[\bar{\nabla}\hat{\boldsymbol{S}}-\frac{1}{3}\bar{\nabla}\left(\bar{\nabla}\boldsymbol{V}\cdot\hat{\boldsymbol{E}}\right)\right]+\left(1-\frac{1}{\mathrm{Pr}}\right)\mu\boldsymbol{V}\bar{\nabla}\frac{|\boldsymbol{V}|^2}{2}-\frac{2}{3}\frac{\gamma-1}{\gamma}\mu|\boldsymbol{V}|^2\bar{\nabla}\boldsymbol{V}}{R\left(\rho_\infty(\boldsymbol{V}\cdot\boldsymbol{V}_\infty)-\frac{\mu}{\mathrm{Pr}}\boldsymbol{V}\bar{\nabla}\boldsymbol{V}\right)}$$

It should be noted that this expression significantly simplifies neglecting viscous effects far awy from circumfluent bodies in high speed flows:

$$\frac{T}{T_\infty}=1+\frac{\gamma-1}{2}\mathrm{M}_\infty^2\left(1-\frac{|\boldsymbol{V}|^2}{|\boldsymbol{V}_\infty|^2}\right).$$

The above expression could also be obtained via assumption of total enthalpy conservation. Corresponding mistake could be estimated from the following expression $\delta T/T_\infty=(\gamma-1)V_p^3\delta V_p\left(4\rho_p a_p^2\xi/9\mu(T)\right)^2/c_\infty^2$.

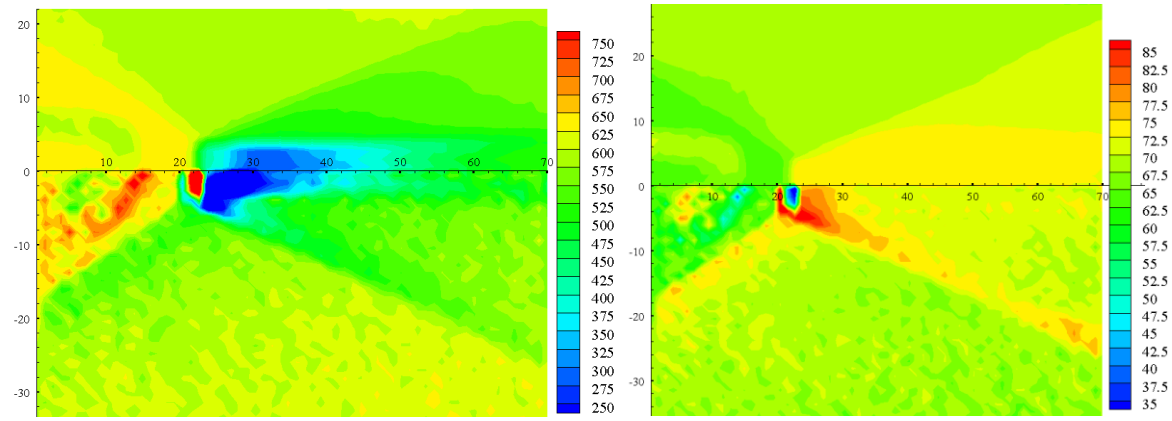

Fig. 3. Results for PIV data correction at high speed. On the left: above – particles' velocity field, below – gas velocity field (using correction on aerosol flow nonequilibrium); on the right: above – temperature determination via particles' velocity field processing, below: temperature determination via gas velocity (corrected particles velocity) determination.

The methods considered above were used to determine the gas parameters (carrier phase) of the aerosol flow by the particle velocity distribution (dispersed phase) obtained by PIV method under the conditions of the experiment in TsNIIMash supersonic wind tunnel [7]. The reflection of a conical shock wave (SW) from the symmetry axis was investigated in the experiment. The experiment was carried out in in a supersonic wind tunnel of continuous action with a flat nozzle and a working part of 0.6×0.6×2.8 m at number of M = 4. The pressure of the flow in the working part was ≈ 0.01 bar., the stagnation temperature was – 5° C, the mass and volumetric flow rate of the gas were ≈ 5 kg/s and 250 m^3/s, respectively. The tracer pictures were recorded with an optical magnification factor of 0.034 mm/pix, and the final spatial resolution of the particles velocity field was ≈ 0.8 vector/mm.
Fig. 3 shows results of particle and gas velocity distribution (left part of the figure) and temperature field distribution estimation (on the top without taking in account phase velocities' nonequilibrium, in the bottom using formula of gas velocity vector field determination via PIV correction method. The described above considerations may be used for molecular clusters internal relaxation phenomena determination as well as gas molecules' dissociations as well as ionization processes estimation.

5 CONCLUSION AND ACKNOWLEDGEMENT

Original approaches in mathematical and numerical simulation of nonspherical shape particles' dynamics in nonuniform flows are developed. Results of shape influence on trajectories' stochastic and spreading of nonspherical bodies in gradient flows are obtained. Mathematical models of the nonspherical particles motion were proposed. A concept of orientation force and complex shape bodies scattering coefficient are introduced. Algorithms for determination gas parameters via particles' motion analysis are developed.

The work is supported by Russian Fund for Basic Research (project No 18-31-00485).

References

1. Nilamdeen S. and Habashi W.G. Multiphase approach toward simulating ice crystal ingestion in jet engines. J. Propulsion and Power. V. 27, No. 5. 959-969. (2011).
2. Amelyushkin, I.A. and Stasenko, A.L.: Interaction of supercooled droplets and nonspherical ice crystals with a solid body in a mixed cloud. CEAS Aeronautics Journal. V. 9, Issue 4, 711-720. (2018).
3. Njobuenwu D.O. and Fairweather M. Dynamics of single, non-spherical ellipsoidal particles in a turbulent channel flow. Chem. Engineering Science. V. 123. 265-282. (2015).
4. Jeffery G.B. The motion of ellipsoidal particles immersed in a viscous fluid. Proc. Roy. Soc. A. Vol. 102. 161-179. (1922).
5. Amelyushkin, I.A. and Stasenko, A.L. Interaction of gas flow carrying nonspherical microparticles with transversal cylinder. J. Phys. Engineering, V. 91, No. 3, 307-318. (2018)
6. Amelyushkin, I.A. Mathematical models and optical investigation of two phase flows in wind tunnels. Proceedings from the 30th Congress of the International Council of the Aeronautical Sciences ICAS-2016 25th–30th September, Daejeon, Korea, 1-5. (2016)
7. Amelyushkin I.A. Ganiev Yu.H., Gobyzov O.A., Lipnitsky Yu.M., Lozhkin Yu.F. and Filippov S.E. nonequilibrium aerosol flow in supersonic wind tunnel. TsAGI Science journal V. 1. 53-71 (2018).
8. Amelyushkin I.A. Supercooled water crystallization in a problem of ice accretion // Journal of Visualization of mechanical processes. V. 4, Issue 1. 1-18. (2016).
9. Amelyushkin I.A. and Stasenko A.L. Interaction of aerosol flow's nanodroplets with a solid body. Nanostructures. Mathematical physics and simulation– V. 14. – № 2. – 5-23 (2016)
10. Eisenschitz R., London F. Über das Verhältnis der van der Waalsschen Kräfte zu den homöopolaren Bindungskräften. Zeitschrift für Physik, 60. – 7. S. 491-457. (1930).